ON THE SENSITIVITY OF THE NORMALIZED DIFFERENCE SNOW INDEX TO METAMORPHIC CHANGES ELICITED IN DRY AND WET SNOWPACKS

Gladimir V.G. Baranoski and Petri M. Varsa

Natural Phenomena Simulation Group, School of Computer Science, University of Waterloo
200 University Ave., Waterloo, Ontario, Canada N2L 3G1

ABSTRACT

Alterations in seasonal snow covers can have profound effects not only on the planet's climate, biodiversity and fresh water supplies, but also on the occurrence of natural hazards like floods and avalanches. The mapping and monitoring of these alterations often rely on the calculation of spectral indices such as the NDSI (normalized difference snow index). Despite the extensive use of the NDSI in remote sensing applications, several aspects related to its sensitivity to changes in snow characteristics remain to be broadly unveiled. These changes can take place during environmentally-induced metamorphic processes, which are being accentuated by increasing global warming conditions. In this work, we systematically examine the impact that concomitant metamorphic changes on key nivological characteristics, namely grain size and density, can have on the NDSI of snowpacks with varying liquid water contents and irradiated from distinct light incidence directions. Our investigation is carried out through controlled *in silico* experiments conducted using a first-principles simulation framework supported by *in situ* measured data obtained from natural snowpacks.

Index Terms— snow, spectral index, metamorphism.

1. INTRODUCTION

The reliable mapping and monitoring of seasonal snow covers are essential for a wide range of studies with pivotal importance for ecological sustainability and human safety, from biodiversity analysis, hydrological modeling and climate change predictions [1, 2] to flood forecasting and avalanche warning [3, 4]. The snowpacks forming these covers undergo continuous environmentally-induced transformations, collectively known as seasonal snow metamorphism [5]. Through successive metamorphic processes, such as sublimation, melting, settling and freezing, key nivological characteristics of snowpacks can change considerably [6, 7, 8], leading to variations in their spectral responses [9, 10]. The detection and correct interpretation of these alterations, in turn, are instrumental for the effective assessment of snow covers increasingly affected by global warming conditions [11, 12].

Thanks to NSERC (grant 108339) for funding.

The remote assessment of snow covers primarily involves airborne sensors with reflectance bands in the visible (VIS) and shortwave-infrared (SWIR) spectral regions [12, 13]. Reflectance values acquired at these bands are then used to calculate spectral indices. Among these indices, the normalized difference snow index (NDSI, ranging from -1 to 1) [14] is arguably the most extensively employed in this area [2, 12, 15, 16]. Its formulation is based on the high and low reflectance values of snow in the VIS and SWIR regions, respectively [13]. Thus, changes in the nivological characteristics affecting snow spectral responses are translated to variations in the calculated NDSI values. The appropriate interpretation of these variations can then be used to support the remote study of snowy landscapes and complement ground-based observations of their alterations over time [1, 8, 12, 17].

Metamorphic processes are known to lead to significant increases in the grain size and density of snowpacks [4, 6, 7, 18]. Although a myriad of studies have been conducted on the effects of grain size on snow reflectance [9, 10, 16, 19], the combined effects of grain size and density changes on the NDSI have not been object of comprehensive examinations to date, specially considering wet conditions.

These nivological characteristics are difficult to be controlled during fields studies of snow metamorphism [4, 18]. Laboratory studies, on the other hand, often rely on artificially prepared snow samples whose characteristics can considerably diverge from those of natural samples [10]. Computational (*in silico*) studies, albeit representing a viable alternative, are bound by the intrinsic limitations of the employed abstract representation of a complex granular material like snow.

In this paper, we investigate the effects that metamorphism elicited changes in the grain size and density of snowpacks, in both dry and wet conditions, can have on their corresponding NDSI values calculated for different angles of light incidence. To overcome the aforementioned difficulties of *in situ* experiments, we employ an *in silico* approach supported by measured data obtained from natural snowpacks [20]. Our investigation is carried out using a first-principles model for light interactions with snow, known as SPLITSnow (*SP*ectral *LI*ght *T*ransport in *Snow*), that explicitly accounts for its particulate nature in order to output high-fidelity radiometric data for different experimental scenarios [21, 22].

2. INVESTIGATION FRAMEWORK

For the *in silico* experiments described in this work, we selected two distinct virtual snow samples, henceforth referred to as samples I and II. Their characterizations were based on actual snow samples (from snowpacks located on the Norwegian Svalbard archipelago, in the Arctic) with negligible liquid water and impurity contents. These samples' nivological descriptions were made available through the SISpec (Snow and Ice Spectral) library along with their respective measured reflectance curves, which were obtained *in situ* [20]. More precisely, these samples, identified as SISpec S6 and S195, were respectively employed to guide the selection of plausible values (Table 1) for the parameters used in the characterization of the virtual samples I and II. For conciseness, more detailed information about the inferences leading to the selection of these values is provided elsewhere [23].

Table 1. Parameter values employed in the characterization of the snow virtual samples considered in this investigation.

	Samples	
Parameters	**I**	**II**
Grain size range (μm)	200–300	150–800
Temperature ($^{\circ}C$)	-8	-3
Thickness (cm)	18	10
Density (kg/m^3)	360	340
Facetness range	0.05–0.25	0.1–0.4
Facetness mean	0.15	0.25
Facetness standard deviation	0.075	0.1
Sphericity range	0.7–0.9	0.9–0.97
Sphericity mean	0.8	0.935
Sphericity standard deviation	0.1	0.05

In our simulations, snow grains are described as prolate spheroids with a semi-major axis equal to b and a semi-minor axis related to b by the grains' sphericity ($\Psi \in [0..1]$, with Ψ equal to 1 yielding perfectly spherical grains) [21], which is represented by a random variable with a probability distribution (PD) previously employed for particulate materials [21]. Thus, the size of a grain corresponds to $2b$ [24], with b being associated with a random variable with a uniform PD. Similarly, the grains' facetness ($f \in [0..1]$, with f equal to zero yielding perfectly smooth grains) is represented by a random variable with a normal PD [21].

We considered the virtual samples subjected to different metamorphic stages (A, B and C). These stages are associated with incremental changes in the samples' grain size and density, with the latter being linked to their porosity [22]. Based on empirical observations reported in the literature [4, 5, 6, 8], we considered distinct increments for the average grain size and density, namely 50% and 25%, respectively. Given the particular features of the reference samples (*e.g.*, composed of rounded grains), it was assumed that they had already been subjected to some degree of metamorphism. Accordingly, we considered the samples characterized by the parameter values presented in Table 1 to be in stage B. For stages A and C, we also considered the same default values presented in Table 1, with the exception of the grain size range and density parameters whose values were respectively reduced and increased using the aforementioned increments. The values assigned to the samples' grain size range and density with respect to each metamorphic stage are presented in Table 2.

Table 2. Values assigned to the grain size range (grs) and density (D) parameters employed in the characterization of the snow virtual samples at their distinct metamorphic stages.

	Sample I		**Sample II**	
Stages	gsr (μm)	D (kg/m^3)	gsr (μm)	D (kg/m^3)
A	100-234	288	50-584	272
B	200-300	360	150-800	340
C	300-450	450	425-1000	425

We note that, although the grains' sphericity and facetness may also incrementally change during ongoing, advanced stages of metamorphism, these changes are likely to be relatively small in these stages [5]. Thus, their impact on the magnitude of snow reflectance is expected to be minor in these cases [21, 25]. For this reason, and considering the scarcity of supporting quantitative information about the metamorphic variations of these parameters, we elected to keep them fixed during our simulations, and to leave the investigation of their impact on the NDSI to future work.

To extend our scope of observations, we also randomly varied (within physically valid limits [5]) the width of the grain size ranges assigned to stages A and C of each virtual snow sample (Table 2). It is also worth mentioning that, to the best of our knowledge, quantitative information about this variable is not readily available in the literature either.

Our controlled *in silico* experiments consisted in computer simulations with the purpose of computing directional-hemispherical reflectance curves for the virtual snow samples at their distinct metamorphic stages. Reflectance values obtained from these curves were then used to calculate the NDSI values for each sample at each metamorphic stage.

The simulations were conducted using SPLITSnow [21, 22] and considering a spectral resolution of 10 nm, with 10^6 incident rays per wavelength. In order to expand the dimensionality of our investigation, we also incrementally varied the angle of light incidence (θ) and the samples' water saturation ($S \in [0..1]$ representing the fraction of a sample's pore space occupied by liquid water) during our simulations. This also enabled us to account for the putative impact of these parameters on the samples' reflectance and, consequently, on the calculated NDSI values [25, 26]. We note, however, that the modeled reflectance values employed in this work, unless otherwise stated, were obtained considering a normal angle of incidence ($\theta = 0^{\circ}$) and the samples in a dry state ($S = 0$).

To calculate the NDSI values associated with each *in silico* experiment described in this work, we employed the following formula [14]:

$$NDSI = \frac{\rho(560) - \rho(1650)}{\rho(560) + \rho(1650)}, \quad (1)$$

where $\rho(\lambda)$ denotes the reflectance value obtained at the wavelength λ (in nm). It is worth mentioning that different versions of this formula can be found in related works [1, 12, 17, 26]. However, as stated by Riggs *et al.* [13], the selection of bands for calculating the NDSI is guided by the sensor(s) being used in a given study, and this spectral index is relatively insensitive to the exact location of the sampled wavelengths within the VIS and SWIR selected bands.

Lastly, to facilitate the reproducibility of our findings, we made the SPLITSnow model accessible for online use [27]. Furthermore, all supporting datasets, such as the spectral refractive indices for ice and water, employed in this investigation are openly available in a dedicated data repository [28].

3. RESULTS AND DISCUSSION

In order to establish reliable baselines for our *in silico* experiments, we computed the reflectance curves for samples I and II using the default parameter values present in Table 1. We then compared the modeled curves with measured curves provided for the SISpec samples [20] used as references. These comparisons, depicted in Fig. 1, reveal a close agreement between the modeled and measured curves. This observation is corroborated by the low root-mean-square errors ($rmse$) calculated for the modeled curves computed for samples I ($rmse = 0.0168$, or 1.68%) and II ($rmse = 0.0176$, or 1.76%) with respect to their measured counterparts.

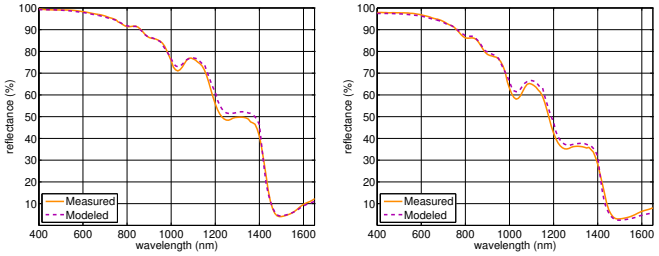

Fig. 1. Comparison of measured and modeled reflectance curves obtained for samples I (left) and II (right) considering the default parameter values presented in Table 1.

In Fig. 2, we present the graphs depicting the reflectance curves obtained for the virtual samples considering the incremental increases in their grain size ranges and densities associated with their metamorphic stages A, B and C (Table 2). As noted in the literature [9], although the overall shape of the reflectance curves remains the same as metamorphism progresses, their magnitude with respect to distinct spectral regions varies. More precisely, as it can observed

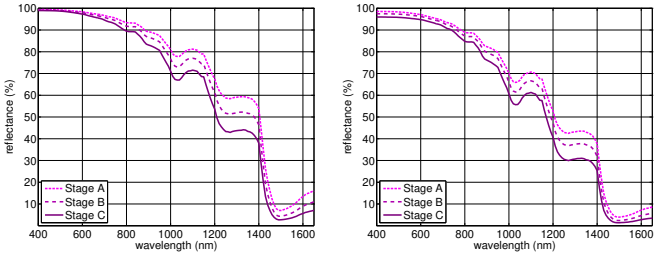

Fig. 2. Modeled reflectance curves obtained for samples I (left) and II (right) with respect to the metamorphic stages A, B and C (Table 2).

in Fig. 2, the overall magnitude of the reflectance curves decreased from stage A to B, and from B to C. This trend is consistent with the inverse relationship of snow reflectance and grain size, notably when this granular material is subjected to metamorphism, with larger grains leading to lower reflectance values [10]. The larger differences between the curves in 700-1300 nm region are also consistent with reported observations indicating that snow reflectance in this spectral region is highly sensitive to grain size variations [19].

On the other hand, while density increases are also likely to lead to reflectance decreases in the 700-1300 nm region [29], they may prompt reflectance increases in the 400-700 nm region [30]. It is worth noting that the connections between density and snow spectral responses are still not well-established. Indeed, reported inferences about these connections [30] are largely based on average reflectance values (calculated from measurements over the entire 350-2800 nm spectral domain [29]), rather than on specific reflectance values obtained for distinct spectral regions (*e.g.*, VIS or SWIR). Nonetheless, the smaller differences among the curves obtained for sample I (with the lower grain size and larger density values) in the 400-700 nm region and larger differences in the 700-1300 nm region are in line with the empirical observations mentioned above.

In Fig. 3, we present plots depicting the NDSI values calculated for the virtual samples at each metamorphic stage, and considering increasing angles of incidence. As it can be observed in these plots, the depicted NDSI trends were directly correlated to the metamorphic stages, with higher NDSI values being obtained for the stages associated with the larger grain sizes and densities. It can also be noted that these trends are markedly nonlinear. More specifically, for small deviations in the angle of incidence ($0° \leq \theta \leq 15°$), the variations in the NDSI values were minor. However, as the angle of incidence increases, the NDSI values become noticeably lower. This can be attributed to a significant nonlinear reflectance increase in the SWIR region and a minor reflectance increase in the VIS region. Thus, the numerator of Eq. 1 becomes smaller while its denominator becomes progressively larger, yielding lower NDSI values. Incidentally, similar reflectance variations were observed in simulations conducted using a distinct modeling approach [9].

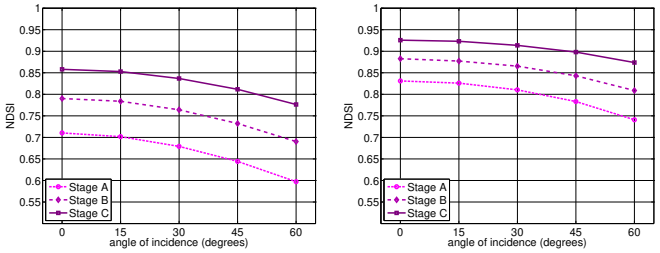

Fig. 3. NDSI values computed for samples I (left) and II (right) with respect to each metamorphic stage (Table 2) and considering increasing angles of incidence (θ).

In Fig. 4, we present plots depicting variations in the NDSI values calculated for the selected samples at their metamorphic stages (A, B and C) as their water saturation (S) values are increased. As it can be noted in these plots, the increase in the samples' water saturation led to a near linear increase in the NDSI values. This trend may be explained by the impact that the presence of liquid water can have on light attenuation mechanisms affecting snow reflectance [21]. By reducing the refractive index differences between the grains and their surrounding medium, it reduces the probability of light being reflected by the grains while increasing the probability of light being refracted by them. Additionally, it increases the probability of SWIR light being absorbed (while traversing a snow sample) in comparison with VIS light since the extinction coefficient of water is considerably higher in the SWIR region [21]. The net effect of these mechanisms is a trend toward a reflectance increase in the VIS region, and a decrease in the SWIR region. Hence, the numerator in Eq. 1 tends to increase while the denominator tends to decrease, yielding higher NDSI values.

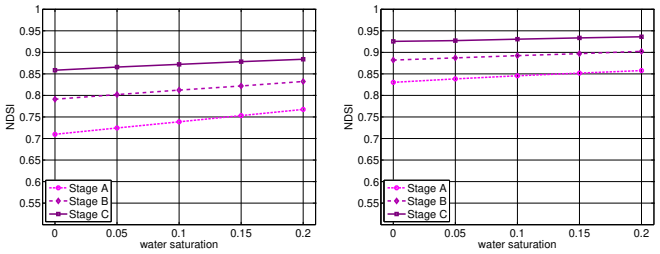

Fig. 4. NDSI values computed for samples I (left) and II (right) with respect to the each metamorphic stage (Table 2) and considering increasing water saturation (S) values.

Our findings indicate that snowpack changes elicited by metamorphic processes can lead to significant NDSI variations. We remark that our *in silico* experiments were conducted considering incremental increases in the samples grain size ranges and densities. During actual observation campaigns, the reflectance measurements required for NDSI calculation can be obtained over an extended period of time, during which the presence of liquid water may also change. Accordingly, the observed NDSI differences may become even more pronounced in these situations. This aspect is illustrated in the graphs presented in Fig 5. Given the importance of reliably mapping and monitoring snow covered landscapes [2, 13, 15, 17], notably those located in geographical regions more susceptible to accentuated warming conditions affecting snow metamorphic processes [1, 11, 12], it is essential to properly account for the combined impact that alterations in different snow characteristics can have on the spectral indices, such as the NDSI, extensively employed in these tasks.

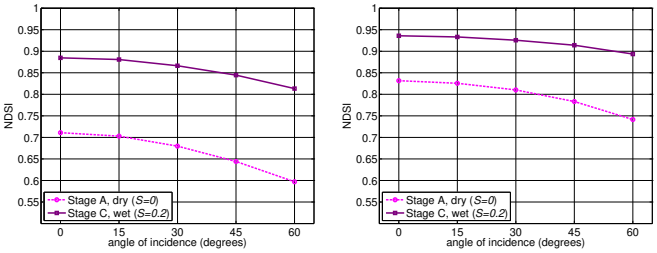

Fig. 5. Comparison of NDSI values computed for samples I (left) and II (right) considering the boundary cases of this investigation: stage A, dry ($S = 0$) and stage C, wet ($S = 0.2$).

4. CONCLUSION AND FUTURE WORK

Although the NDSI and grain size relationship has been examined in the literature [15, 16, 25], empirical evidence regarding the NDSI sensitivity to progressive metamorphic changes in both grain size and density, leading to significant increases in their magnitudes, is scarce. In this work, we aimed to address this evidence gap by investigating the impact of these changes, considering not only distinct angles of light incidence, but also varying water saturation levels.

To our knowledge, the combination of these experimental dimensions has not been systematically examined in previous works involving NDSI calculations for snow at different metamorphic stages. The trends observed in our work indicate a noticeable increase in the NDSI as a snowpack becomes progressively denser and composed of larger grains. Moreover, the NSDI values associated with these changes decrease nonlinearly for relatively large angles of incidence, and increase nearly linearly with higher water saturation levels.

Clearly, the correct interpretation of NDSI variations, particularly those associated with the accentuated metamorphism of snow covers subjected to increasing warming conditions, requires a comprehensive understanding about the processes leading to alterations in the snow spectral responses. The pursuit of this overarching objective will likely involve an intensification of interdisciplinary research efforts in this area.

As future work, we plan to further expand the scope of our investigation by including more samples and examining the NDSI sensitivity to larger grain shape changes that can occur during early metamorphic stages. We also intend to examine the effects of aggregated variations in the water and impurity contents of metamorphic snow samples on the NDSI.

5. REFERENCES

[1] B. Busseau, A. Royer, A. Roy, A. Langlois, and F. Dominé, "Analysis of snow-vegetation interactions in the low Artic-Subartic transition zone (northeastern Canada)," *Phys. Geogr.*, vol. 38, no. 2, pp. 159–175, 2017.

[2] C. Poussin, P. Timoner, B. Chatenoux, G. Giuliani, and P. Peduzzi, "Improved Landsat-based snow cover mapping accuracy using a spatiotemporal NDSI and generalized linear mixed model," *The Sci. Remote Sens.*, vol. 7, pp. 100078:1–13, 2023.

[3] M. Lehning, P. Bartelt, B. Brown, C. Fierz, and P. Satyawali, "A physical SNOWPACK model for the Swiss avalanche warning: Part II snow microstructure," *Cold Reg. Sci. Technol.*, vol. 35, pp. 147–167, 2002.

[4] L. Leppänen, A. Kontu, J. Vehviläinen, J. Lemmetyinen, and J. Pulliainen, "Comparison of traditional and optical grain-size field measurements with SNOWPACK simulations in a taiga snowpack," *J. Glaciol.*, vol. 61, no. 225, pp. 151–162, 2015.

[5] S.C. Colbeck, "An overview of seasonal snow metamorphism," *Rev. Geophys. Space Ge.*, vol. 20, no. 1, pp. 45–61, 1982.

[6] R.W. Gerdel, "Penetration of radiation into the snow pack," *AGU Trans.*, vol. 20, no. 3, pp. 366–374, 1948.

[7] H. Curl Jr., J.T. Hardy, and R. Ellermeier, "Spectral absorption of solar radiation in Alpine snowfields," *Ecology*, vol. 53, no. 6, pp. 1189–1194, 1972.

[8] S. Gerland, J. Winther, J.B. Øbaek, G.L. Liston N.A., Øristland, A. Blanco, and B. Ivanov, "Physical and optical properties of snow covering Arctic tundra and Svalbard," *Hydrol. Processes*, vol. 13, pp. 2331–2343, 1999.

[9] B.J. Choudhury and A.T.C. Chang, "On the angular variation of solar reflectance of snow," *J. Geophys. Res.*, vol. 86, no. C1, pp. 465–472, 1981.

[10] T. Nakamura, O. Abe, T. Hasegawa, R. Tamura, and T. Ohta, "Spectral reflectance of snow with a known grain-size distribution in successive metamorphism," *Cold Reg. Sci. Technol.*, vol. 32, pp. 13–26, 2001.

[11] P. Niittynen, R.K. Heikkinen, and M. Luoto, "Snow cover is a neglected driver of Arctic biodiversity loss," *Nat. Clim. Change*, vol. 8, pp. 997–1003, 2018.

[12] J. Zheng, G. Jia, and X. Xu, "Earlier snowmelt predominates advanced spring vegetation greenup," *Agr. Forest Meteorol.*, vol. 315, pp. 1245:1–19, 2022.

[13] G.A. Riggs, D.K. Hall, and M.O. Román, "Overview of NASA's MODIS and Visible Infrared Imaging Radiometer Suite (VIIRS) snow-cover Earth system data records," *Earth Syst. Sci. Data*, vol. 9, pp. 765–777, 2017.

[14] G.A. Riggs, D.K. Hall, and V.V. Salomonson, "A snow index for the Landsat thematic mapper and moderate resolution imaging spectroradiometer," in *International Geoscience and Remote Sensing Symposium - IGARSS*, 1994, pp. 1942–1944.

[15] R. Kour, N. Patel, and A.P. Krishna, "Assessment of relationship between snow cover characteristics (SGI and SCI) and snow cover indices (NDSI and S3)," *Earth Sci. Inf.*, vol. 8, pp. 317–326, 2015.

[16] Y. Wang, Y. Chen, P. Li, Y. Zhan, R. Zou, B. Yuan, and X. Zhou, "Effect of snow cover on detecting spring phenology from satellite-derived vegetation indices in Alpine grasslands," *Remote Sens.*, vol. 14, pp. 5725:1–24, 2022.

[17] S. Härer, M. Bernhardt, M. Siebers, and K. Schulz, "On the need for a time- and location-dependent estimation of the NDSI threshold value for reducing existing uncertainties in snow cover maps at different scales," *The Cryosphere*, vol. 12, pp. 1629–1642, 2018.

[18] H. Wen, W. Wen shou L. Ming-zhe, L. Heng, H. Xi, and Z. Yan-wei, "Metamorphism and microstructure of seasonal snow: single layer tracking in Western Tianshan, China," *J. Mt. Sci.*, vol. 11, no. 2, pp. 496–506, 2014.

[19] A.W. Nolin and J. Dozier, "Estimating snow grain size using AVIRIS data," *Remote Sens. Environ.*, vol. 44, pp. 231–238, 1993.

[20] R. Salvatori, R. Salzano, M. Valt, R. Cerrato, and S. Ghergo, "The collection of hyperspectral measurements on snow and ice covers in Polar regions (SISpec 2.0)," *Remote Sens.*, vol. 14, pp. 2213:1–14, 2022.

[21] P.M. Varsa, G.V.G. Baranoski, and B.W. Kimmel, "SPLITSnow: A spectral light transport model for snow," *Remote Sens. Environ.*, vol. 255, pp. 112272:1–20, 2021.

[22] P.M. Varsa, *A First-Principles Framework for Simulating Light and Snow Interactions*, Ph.D. thesis, University of Waterloo, Ontario, Canada, March 2025.

[23] G.V.G. Baranoski and P.M. Varsa, "Environmentally induced snow transmittance variations in the photosynthetic spectral domain: Photobiological implications for subnivean vegetation under climate warming conditions," *Remote Sens.*, vol. 16, no. 927, pp. 1–23, 2024.

[24] C. Fierz, R.L. Armstrong, Y. Durand, P. Etchevers, E. Greene, D.M. McClung, K. Nishimura, P.K. Satyawali, S., and Sokratov, "The international classification for seasonal snow on the ground," Tech. Rep. IHP-VII N°83, UNESCO, International Hydrological Programme, Paris, France, 2009.

[25] W. Ji, X. Hao, D. Shao, Q. Yang, J. Wang, H. Li, and G. Huang, "A new index for snow/ice/ice-snow discrimination based on BRDF characteristic observation data," *J. Geophys. Res.-Atmos.*, vol. 127, pp. 1–17, 2022.

[26] G. Wang, L. Jiang, C. Xiong, and Y. Zhang, "Characterization of NDSI variation: implications for snow cover mapping," *IEEE T. Geosci. Remote*, vol. 60, pp. 4304318:1–18, 2022.

[27] Natural Phenomena Simulation Group (NPSG), *Run SPLITSnow Online*, School of Computer Science, University of Waterloo, Ontario, Canada, 2021, Link to model interface: http://www.npsg.uwaterloo.ca/models/splitsnow-i.php.

[28] Natural Phenomena Simulation Group (NPSG), *Snow Data*, School of Computer Science, University of Waterloo, Ontario, Canada, 2020, http://www.npsg.uwaterloo.ca/data/snow.php.

[29] C.F. Bohren and R.L. Beschta, "Snowpack albedo and snow density," *Cold Reg. Sci. Technol.*, vol. 1, no. 1, pp. 47–50, 1979.

[30] D.K. Perovich, "Light reflection and transmission by a temperate snow cover," *J. Glaciol.*, vol. 53, no. 181, pp. 201–210, 2007.